PHYSICAL REVIEW B **66**, 161305(R) (2002)

Flux-quantum-modulated Kondo conductance in a multielectron quantum dot

C. Fühner,* U. F. Keyser, and R. J. Haug
Institut für Festkörperphysik, Universität Hannover, Appelstrasse 2, 30167 Hannover, Germany

D. Reuter and A. D. Wieck
Lehrstuhl für Angewandte Festkörperphysik, Ruhr-Universität Bochum, 44780 Bochum, Germany

(Received 10 July 2002; published 4 October 2002)

We investigate a lateral semiconductor quantum dot with a large number of electrons in the limit of strong coupling to the leads. A Kondo effect is observed and can be tuned in a perpendicular magnetic field. This Kondo effect does not exhibit Zeeman splitting. It shows a modulation with the periodicity of one flux quantum per dot area at low temperatures. The modulation leads to a strikingly regular stripe pattern for a wide range in magnetic field and number of electrons.

DOI: 10.1103/PhysRevB.66.161305 PACS number(s): 72.15.Qm, 73.21.La, 73.23.Hk, 73.40.Gk

The Kondo effect[1] in semiconductor quantum dots[2] has been the subject of numerous theoretical and experimental investigations in recent years. Originally, Kondo developed his theory to explain the increased resistivity in bulk metals due to magnetic impurities at low temperatures. Later, this theory was also applied to quantum dots,[3,4] leading to first successful experiments in semiconductor dots which allowed a controlled and detailed study of the Kondo phenomenon.[5] These early experiments were interpreted in terms of the ordinary Anderson impurity model,[6] describing the interaction of a singly occupied, spin-degenerate level—realized within the quantum dot—with conduction-band electrons. Deviations were attributed to nearby levels present in real dots.[7] Subsequently, the quantum dots have been tuned into more complex regimes, showing Kondo behavior beyond the simple spin-1/2 Anderson impurity model. For a quantum dot with many electrons, the occurrence of Kondo physics depends on the exact form of the multielectron spectrum including Hund's rule.[8] In a magnetic field, the ground state of such a system and thus the ability to show a Kondo effect is modified. Unpaired spin configurations at the edge may lead to a Kondo effect.[9,10] Furthermore, multiple correlated electrons on the dot may couple in a $S \geqslant 1$ state which may also exhibit Kondo physics. This was demonstrated in magnetically tuned degeneracies between singlet and triplet states[11] (also observed in carbon nanotubes[12]) and is now well understood.[13–15] Another deviation from the Anderson model can be observed when several energy levels of the dot come into play. This happens when either the coupling of the dot to the leads is not small compared to the level spacing anymore[16–19] or when the dot is tuned close to a Coulomb resonance.[20,21] The system then enters the mixed valence regime.

In this work, we study Kondo physics in a rather large lateral quantum dot containing many electrons. While the energies involved in tunneling through dots resembling the Anderson impurity model can be depicted like in Fig. 1(a), the situation in our dot is more like in Fig. 1(b). Due to the larger size of our dot, the internal level spacing ΔE is comparably small, whereas the coupling Γ to the leads is strong so that $\Gamma \approx \Delta E$. Kondo as well as mixed valence effects should play a role. In addition, the large number of electrons in our dot provides electronic ground states complex enough to allow a variety of Kondo effects like a singlet-triplet Kondo effect or even more complicated ones. These ground states are tuned in a magnetic field.

We fabricated our sample from a modulation doped GaAs/AlGaAs heterostructure which forms a two-dimensional electron gas 57 nm below the surface with an electron density of $n = 3.7 \times 10^{15}$ m^{-2} and a low-temperature mobility of $\mu = 130$ m^2/V s. After etching and contacting a standard Hall bar structure using optical lithography, we applied electron beam lithography to pattern six metallic gate electrodes (6 nm Cr, 25 nm Au) across the Hall bar (inset in Fig. 2). From the scanning electron microscopy (SEM) image a geometric dot diameter of 380 nm is deduced. Taking into account the depletion length of our split gates, we obtain an electronic diameter of $d_{el} \approx 250$ nm resulting in a dot with $N \approx 180$ electrons. From our dot geometry we estimate a confinement-induced single particle level spacing of $\Delta E \approx 2\hbar^2/m^* r^2 = 150$ μeV. Differential conductance measurements were carried out in a ^{3}He-^{4}He dilution refrigerator with a base temperature of 20 mK, using standard lock-in technique. From the saturation of peak widths in temperature dependent Coulomb blockade measurements we determine the minimal electronic temperature to be $T_0 \lesssim 70$ mK.

The quantum dot is defined by application of negative voltages to the gate electrodes: slightly asymmetric tunnel

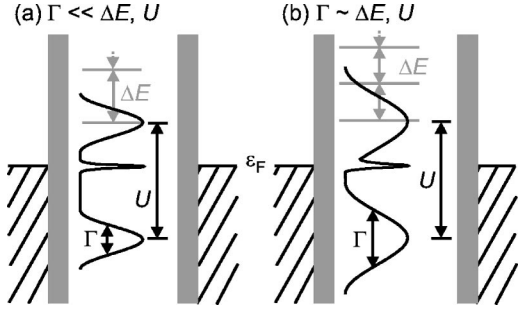

FIG. 1. Schematic energy diagrams of quantum dots with charging energy U, level spacing ΔE, and tunnel coupling Γ. (a) A dot in the Kondo regime with the characteristic narrow resonance in the density of states at the Fermi energy ϵ_F. (b) The situation in our dot, where U, ΔE, and Γ are of similar magnitude.

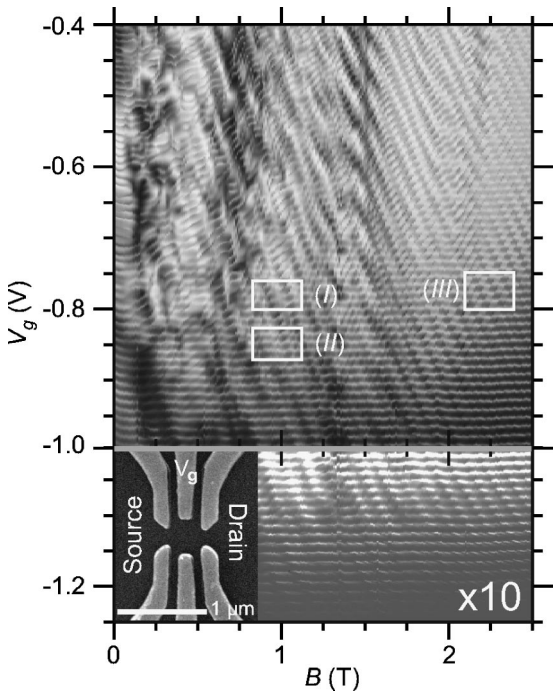

FIG. 2. Gray scale plot of the linear conductance G as a function of plunger gate voltage and perpendicular magnetic field, black corresponds to zero conductance and white to $G=1.8\ e^2/h$. For $V_g<-1$ V, the contrast has been enhanced by a factor of 10. A striking, regular diagonal stripe pattern is visible especially for magnetic fields $B>1$ T. Inset: SEM picture of the Cr/Au gates used to define the quantum dot. The gate marked with V_g is the plunger gate, all other gates are kept at constant voltages.

barriers are created by applying -1.084 V to the left and -1.220 V to the right gate pair. The lower gate in the middle of the structure is kept constant at -1.084 V while the upper one is used as a plunger gate to control the electrostatic potential, increasing the number of electrons on the dot by 75 in varying V_g from -1.250 V to -0.400 V. Due to its proximity to the tunnel barriers the plunger gate strongly influences the coupling of the dot to the leads. For voltages around $V_g\sim-1.2$ V our dot is in the Coulomb blockade regime with high barrier resistances $R_T\gg h/e^2$. For $B=0$ T we find a charging energy of $U\approx600\ \mu$eV from Coulomb blockade diamonds and an intrinsic line width of $\Gamma\approx100\ \mu$eV estimated from temperature dependent measurements of the Coulomb blockade peak width. Near $V_g\sim-1.0$ V a distinct Kondo resonance appears in several consecutive Coulomb blockade diamonds. In this regime, we estimate our line width as approximately $\Gamma\approx250\ \mu$eV and the charging energy $U\approx500\ \mu$eV at $B=0$ T. From excitation spectroscopy measurements we extract a level spacing of $\Delta E\approx100\ \mu$eV in rough agreement with the estimation presented above.

Figure 2 shows an overview of the linear conductance G versus plunger gate voltage V_g and perpendicular magnetic field B. For magnetic fields $B\gtrsim1$ T a diagonal stripe pattern is clearly visible. Similar patterns were observed for several samples. The striking regularity of this pattern vanishes only for low fields and strong coupling (upper left region in the figure) where $G(B,V_g)$ becomes rather complicated. This can be attributed to the increased influence of disorder in this regime. Chaotic effects typical for open quantum dots might also play a role. We will discuss the origin of the regular pattern—a modulated Kondo effect—in Figures 4 and 5 below, but will first focus on its periodicity.

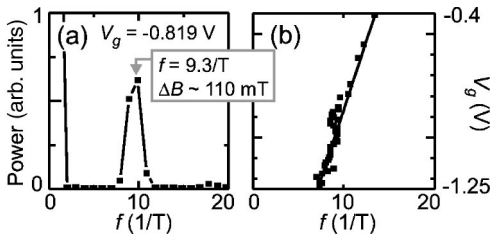

FIG. 3. Analysis of the V_g dependent periodicity of the stripe pattern in Fig. 2 between 1.5 T and 2.5 T, where the pattern is most clearly visible. (a) Fourier transform of one line in Fig. 2 ($V_g=-0.819$ V) along the B axis, showing a distinct peak corresponding to a periodicity of $\Delta B\approx110$ mT. (b) Evaluations like in (a) show a roughly linear variation of the peak position with gate voltage V_g.

The measured conductivity was Fourier transformed along the B axis for several gate voltages V_g. Figure 3(a) shows a typical result of the power spectrum obtained. A clear peak is observed at a frequency of $f=9.3\ \mathrm{T}^{-1}$ corresponding to a periodicity of $\Delta B\approx110$ mT. Each such transformation exhibits such a peak, from which we find a periodicity varying from $\Delta B_1=130$ mT at $V_g=-1.2$ V to $\Delta B_2=75$ mT at $V_g=-0.4$ V. We have identified the periodicity with the addition of one flux quantum to the dot: $N_\phi=1$ flux quanta ϕ_0 added per stripe period lead to dot

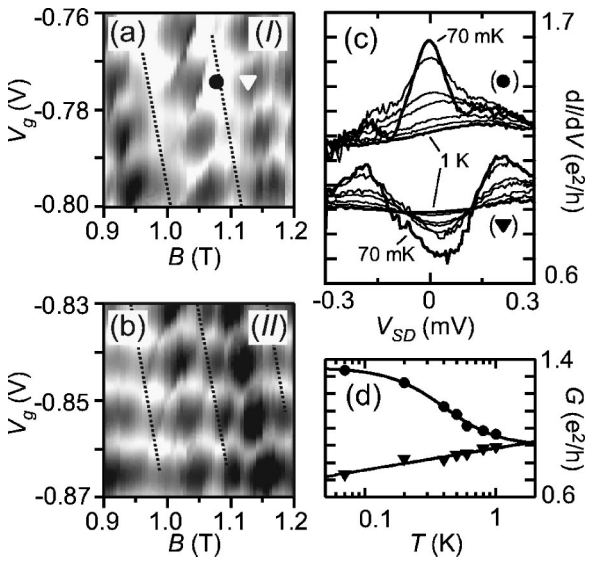

FIG. 4. (a) and (b), a more detailed view into the regions I and II marked in Fig. 2 with the extrapolated stripe positions highlighted by dotted lines (black corresponds to $G=0.4\ e^2/h$ and white to $1.2\ e^2/h$). (c) Differential conductance vs V_{SD} in high (●) and low (▼) conductance regions marked in (a) for temperatures $T=70$, 200, 400, 500, 600, 800, and 1000 mK. (d) Temperature dependence of linear conductance ($V_{SD}=0$ V) at the positions marked in (a) and corresponding fits.

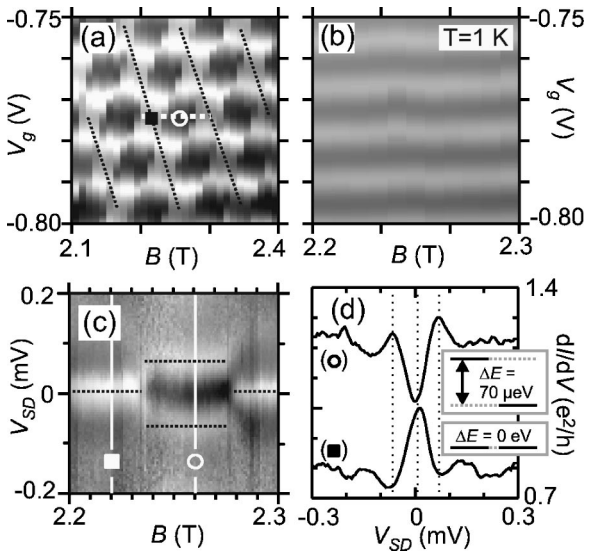

FIG. 5. Analysis of region III from Fig. 2, $B \approx 2.2$ T. (a) The stripe pattern is formed by tiles of increased conductance between Coulomb blockade peaks over a wide parameter range. The black dotted lines illustrate the stripes. (b) At $T=1$ K, the tile pattern in (a) has vanished. (c) Nonlinear magnetoconductance along the white dotted line in (a) in the Coulomb blockade valley at a fixed $V_g=-0.775$ V. Conductance maxima are highlighted with horizontal dotted lines. (d) Cuts as marked in (c). Peak positions are highlighted with dotted lines at $V_{SD}=0$ V and ± 70 μV. The curves are offset for clarity.

diameters $d=2\sqrt{N_\phi \phi_0/\pi \Delta B}$ ranging from 200 nm ($V_g=-1.2$ V) to 265 nm ($V_g=-0.4$ V) which is in good agreement with the value of $d_{el} \approx 250$ nm estimated above from the gate geometry. The smaller diameter for a more negative plunger gate voltage is expected due to an increased depletion. From the calculated diameters we expect a change in the number of electrons on the dot of $\Delta N=87$ electrons which closely resembles $\Delta N=75$ electrons as known from Coulomb blockade. The small difference could be easily attributed to the uncertainty in the charge density n and its unknown exact form in the presence of charged top gates.

The addition of a flux quantum to a many-electron system will change its orbital and spin wave functions for magnetic fields smaller than the extreme quantum limit.[22,23] As an example, McEuen *et al.*[22] observed a redistribution of electrons between different Landau levels within their dot when a flux quantum was added. Thus we can link our stripe period to such redistributions of electrons. In traces of Coulomb peak positions $V_g(B)$ and amplitudes $G(B)$ we observe consistent behavior.

To clarify the origin of the stripe pattern, we will now focus on more detailed measurements in the fairly regular $B \sim 1$ T regime as marked in Fig. 2 by (I). The stripe pattern is made up of regions of enhanced conductance in the Coulomb *blockade* regions [Fig. 4(a)], which together with the Coulomb peaks form tiles of increased conductance. We have performed temperature and source-drain voltage dependent measurements at the marked gate voltage and magnetic-field values to analyze this effect [Fig. 4(c)]. In the high-conductance regions, a zero bias peak is observed (circle in the figure). It vanishes with increasing temperature and disappears at a temperature of $T \approx 1$ K. This zero bias peak is a clear signature of an interaction effect. It can be attributed to the Kondo effect which is illustrated by the characteristic temperature dependence in Fig. 4(d). Due to the high and increasing background conductance it is difficult to determine an exact Kondo temperature T_K. After subtracting the exponential background (triangle), the temperature dependence can be fit by the empirical formula $G(T)=G_0(T_K'^2/(T^2+T_K'^2))^s$ with $T_K'=T_K/\sqrt{2^{1/s}-1}$,[21] from which we extract $T_K \approx 0.4$ K and $s \approx 1$. Although the value of s strongly depends on the other fit parameters, it clearly deviates from $s=0.2$ characteristic for a spin-1/2 system in the Kondo regime. For the low conductance regions, the central Kondo peak is suppressed [Fig. 4(c)]. Here the two small side peaks at ± 170 μeV which are also visible in the high-conductance trace become more prominent. We expect them to be related to a Kondo effect involving inelastic cotunneling through excited states as discussed in Ref. 24. This would be roughly consistent with the level spacing $\Delta E \approx 150$ μeV stated above and also explains the background conductance increasing exponentially with temperature in Fig. 4(d) (triangle). In linear conductance ($V_{SD}=0$ V), the central Kondo peak appears as a high-conductance tile and the absence of a Kondo peak as a low-conductance tile. Stripe and tile patterns can thus be explained with a magnetically modulated Kondo effect.

In the $B \sim 1$ T regime, in some places the situation is not as clear cut and deviations from the regular magnetoconductance pattern are found. In Fig. 4(b) corresponding to region II in Fig. 2, we observe a more honeycomblike structure made up of narrow high-conductance lines between two adjacent Coulomb blockade peaks instead of a high-conductance tile.

Compared to the $B \sim 1$ T regime, for a higher magnetic field, e.g., at $B \sim 2$ T, the stripe pattern is much clearer and extremely regular [Fig. 5(a), corresponding to region III from Fig. 2]. Different from the former, the latter regime extends over a wide range of gate voltage and magnetic field. It consists of alternating tiles of enhanced and suppressed conductance within the Coulomb blockade regions like in region I discussed above. The Kondo effect observed here and thus the pattern itself vanishes totally with increasing temperature [Fig. 5(b)], i.e., at temperatures above $T \approx 0.5$ K only regular Coulomb blockade resonances are observed. From measurements similar to the ones presented in Fig. 4(d) we extract a Kondo temperature of roughly $T_K \approx 0.2$ K. To investigate the nature of the Kondo physics found here, we examine the involved energy scales in V_{SD} dependent conductance measurements along the horizontal dotted line in Fig. 5(a) at a fixed gate voltage [Fig. 5(c)]. We observe a central Kondo peak in high-conductance tiles which is abruptly split into two nearly symmetric peaks in the low-conductance region. At the transition the ground state of the dot and thus the nature of the Kondo state changes. For the two different situations Fig. 5(d) shows two typical differential conductance measurements versus V_{SD} along the vertical lines marked in Fig. 5(c). In the high-conductance/single peak situation the ground state must be

degenerate, i.e., the level splitting must be $\Delta E = 0$ *including* Zeeman energy. In the low-conductance/split peak regime, however, two states with $\Delta E = 70$ μeV (also *including* Zeeman energy) must be involved. This is illustrated in the insets in Fig. 5(d). The single peak situation is clearly inconsistent with the simple model of one electron with spin $S = \pm 1/2$ on a Zeeman split level from which a splitting $\Delta E_Z = g_{GaAs}\mu_B B = 55$ μeV ($|g_{GaAs}| = 0.44$) would be expected. Due to the low ratio $k_B T_K / E_Z = 0.3 < 1$ we should be able to resolve such a splitting. The Kondo states we observe in our strong coupling case must be more complicated than a simple hybridization between leads and one electron on the dot. For example, a two-stage Kondo effect[19,17,18] could be involved, although we have no signature of a suppression of the Kondo effect in the investigated temperature range.

Our result is different from the chessboardlike magnetoconductance pattern investigated previously by Keller *et al.*[9] who observed an alternation between Zeeman split spin-1/2 Kondo peaks in their high-conductance regions and no Kondo effect at all. We attribute this discrepancy to a steeper confinement potential in their reactive ion etched dot and to a lower Kondo temperature and coupling in comparison to our system.

In conclusion, we explored Kondo physics in a large quantum dot with strong coupling to the leads. We observed a flux quantum modulated Kondo effect over a wide parameter range in magnetic field and in the number of electrons in the dot. This Kondo effect needs an explanation that goes beyond the classical spin-1/2 Anderson model.

We thank F. Hohls and U. Zeitler for helpful discussions and help with the measurement setup. We acknowledge discussions with M. Pustilnik and A. Tagliacozzo and financial support by DIP, TMR, BMBF. A. D. W. acknowledges support from SFB491.

*Electronic address: fuehner@nano.uni-hannover.de

[1] J. Kondo, Prog. Theor. Phys. **32**, 37 (1964).
[2] L.P. Kouwenhoven *et al.*, in *Mesoscopic Electron Transport*, edited by L.L. Sohn, L.P. Kouwenhoven, and G. Schön (Kluwer, Dordrecht, 1997), pp. 105–214.
[3] L.I. Glazman and M.E. Raikh, JETP Lett. **47**, 452 (1988).
[4] T.K. Ng and P.A. Lee, Phys. Rev. Lett. **61**, 1768 (1988).
[5] D. Goldhaber-Gordon *et al.*, Nature (London) **391**, 156 (1998); S.M. Cronenwett *et al.*, Science **281**, 540 (1998); J. Schmid *et al.*, Physica B **256**, 182 (1998); F. Simmel *et al.*, Phys. Rev. Lett. **83**, 804 (1999).
[6] P.W. Anderson, Phys. Rev. **124**, 41 (1961).
[7] A.L. Yeyati, F. Flores, and A. Martín-Rodero, Phys. Rev. Lett. **83**, 600 (1999).
[8] J. Schmid *et al.*, Phys. Rev. Lett. **84**, 5824 (2000).
[9] M. Keller *et al.*, Phys. Rev. B **64**, 033302 (2001).
[10] C. Tejedor and L. Martín-Moreno, Phys. Rev. B **63**, 035319 (2001).
[11] S. Sasaki *et al.*, Nature (London) **405**, 764 (2000).
[12] J. Nygård, D.H. Cobden, and P.E. Lindelof, Nature (London) **408**, 342 (2000).
[13] M. Pustilnik, Y. Avishai, and K. Kikoin, Phys. Rev. Lett. **84**, 1756 (2000); M. Pustilnik and L.I. Glazman, Phys. Rev. Lett. **85**, 2993 (2000); M. Pustilnik and L.I. Glazman, Phys. Rev. B **64**, 045328 (2001).
[14] M. Eto and Y.V. Nazarov, Phys. Rev. Lett. **85**, 1306 (2000).
[15] D. Giuliano and A. Tagliacozzo, Phys. Rev. Lett. **84**, 4677 (2000).
[16] A.L. Chudnovskiy and S.E. Ulloa, Phys. Rev. B **63**, 165316 (2001).
[17] W. Hofstetter and H. Schoeller, Phys. Rev. Lett. **88**, 016803 (2002).
[18] W.G. van der Wiel *et al.*, Phys. Rev. Lett. **88**, 126803 (2002).
[19] M. Pustilnik and L.I. Glazman, Phys. Rev. Lett. **87**, 216601 (2001).
[20] T.A. Costi *et al.*, J. Phys.: Condens. Matter **6**, 2519 (1994).
[21] D. Goldhaber-Gordon *et al.*, Phys. Rev. Lett. **81**, 5225 (1998).
[22] P.L. McEuen *et al.*, Phys. Rev. B **45**, 11 419 (1992).
[23] M. Ciorga *et al.*, Phys. Rev. B **61**, R16 315 (2000).
[24] S. de Franceschi *et al.*, Phys. Rev. Lett. **86**, 878 (2001).